

Observation of diffraction with the CMS experiment at the Large Hadron Collider*

Dmytro Volyanskyy^{†‡}
Deutsche Elektronen-Synchrotron DESY
Notkestrasse 85, 22607 Hamburg, Germany

A clear evidence of inclusive diffraction observed by the CMS detector at the Large Hadron Collider in minimum bias events at $\sqrt{s} = 0.9$ TeV, 2.36 TeV is presented. The observed diffractive signal is dominated by inclusive single-diffractive dissociation and can be identified by the presence of a Large Rapidity Gap that extends over the forward region of the CMS detector. A comparison of the data with Monte Carlo predictions provided by PYTHIA6 and PHOJET generators is given. In addition, first observation of the single-diffractive production of di-jets at $\sqrt{s} = 7$ TeV is presented.

PACS numbers:

Keywords: CMS, diffraction

I. PHYSICS MOTIVATION

Diffractive scattering processes attract a lot of interest due to a significant contribution to the total pp cross-section [1]. A proper constraint on the diffractive component is thus essential to improve our understanding of collision data and the pile-up as well as to tune the existing Monte Carlo models of pp interactions at the LHC. In pp collisions, a diffractive process is mainly a reaction $pp \rightarrow XY$, where X and Y can either be protons or low-mass systems which may be a resonance or a continuum state. In all cases, the final states X and Y acquire the energy approximately equal to that of the incoming protons and carry the quantum numbers of the proton as well as are separated by a Large Rapidity Gap (LRG). Diffraction in the presence of a hard scale can be described with perturbative QCD by the exchange of a colorless state of quarks or gluons, whereas soft diffraction at high energies is described in the Regge Theory [2] as a colorless exchange mediated by a specific trajectory, the Pomeron, having the quantum numbers of the vacuum. Two main types of diffractive processes occurring in pp collisions are the single-diffractive dissociation (SD) where one of the protons dissociates and the double-diffractive dissociation (DD) where both protons are scattered into a low-mass system. Another diffractive process that may occur in pp collisions with

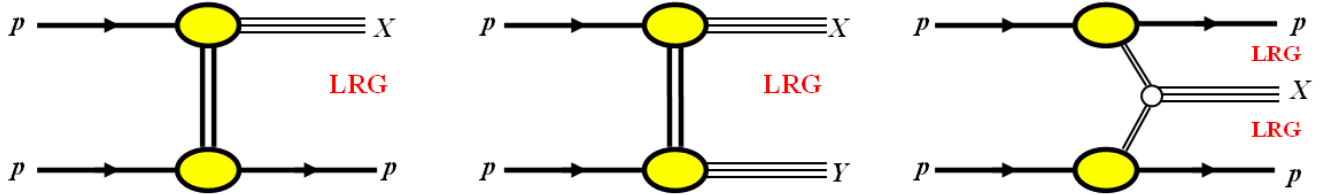


Figure 1: Diagram of the SD reaction $pp \rightarrow pX$ (left), the DD reaction $pp \rightarrow XY$ (middle) and the CD reaction $pp \rightarrow pXp$ (right).

Table I: The estimated cross-sections for different pp interactions at the LHC for $\sqrt{s} = 14$ TeV [1].

Total pp cross-section	$111.5 \pm 1.2^{+4.1}_{-2.1}$ mb
Inelastic, non-diffractive interactions	~ 65 mb
Elastic scattering	~ 30 mb
SD dissociation ($pp \rightarrow pX$)	~ 10 mb
DD dissociation ($pp \rightarrow XY$)	~ 7 mb
CD dissociation ($pp \rightarrow pXp$)	~ 1 mb

[†] on behalf of the CMS collaboration

*Presented at the Workshop on Forward Physics at the LHC (December 12-14, 2010), Manchester, United Kingdom

[‡]Electronic address: Dmytro.Volyanskyy@cern.ch



Figure 2: One of the two HF calorimeters before the installation into the CMS interaction point IP5 (left) and HF wedges during assembly (right).

relatively large cross-section is the central-diffractive dissociation (CD), also known as Double Pomeron Exchange, where the final state includes two incoming protons and one low-mass system created as a result of the interaction between two Pomeron-like objects emitted by the protons. Figure 1 illustrates a sketch for each of these processes and Table I gives the corresponding cross-sections at the LHC for $\sqrt{s} = 14$ TeV.

It is known that the cross-section of hard diffractive processes can be factorized into a hard scattering contribution and a diffractive parton distribution function (dPDF), which contains valuable information about low- x partons. However, the factorization is broken when scattering between spectator partons of the beam particles takes place. This effect is quantified by the so-called rapidity gap survival probability, which can be probed by measuring the ratio of diffractive to inclusive processes with the same hard scale. At the Tevatron, the ratio is found to be $O(1\%)$, whereas theoretical expectations at the LHC vary from a fraction of a percent to up to 30% [3]. A good way to measure this quantity at the LHC is provided by the SD production of W and di-jets, which are hard diffractive processes sensitive to the quark and gluon component of the proton dPDF, correspondingly. A selection of such events at CMS can be performed using the multiplicity distributions of calorimeter towers or tracks in the central region of CMS and calorimeter towers in the forward CMS calorimeters exploiting the fact that diffractive events on average have lower multiplicity in the central region and in the "gap side" than non-diffractive ones. Feasibility studies to detect the SD productions of W [4] and di-jets [5] at CMS showed that the diffractive events peak in the regions of no activity in the forward calorimeters, which is due to the LRG presence.

II. EXPERIMENTAL INSTRUMENTATION

The Compact Muon Solenoid (CMS) experiment built at the Large Hadron Collider is one of the largest scientific instruments ever constructed. The detector has a cylindrical structure with the overall diameter of 15 m, the overall length of 21 m and the total weight of about 12.5 thousands tons and consists of about 76.5 millions of readout channels in total. Its detailed description can be found in [6]. The detector has been designed, constructed and currently operated by the collaboration consisting of more than 3500 scientists from 38 countries. To enhance the physics reach of the experiment the CMS detector includes several calorimeters covering the very forward region of the experiment. This significantly expands the CMS capability to investigate physics processes occurring at very low polar angles and so, provides a valuable tool to study diffractive scattering, low- x QCD, multi-parton interactions and underlying event structure.

One of the forward detectors, which was used in particular to observe diffractive scattering in first minimum bias events, is the Hadronic Forward (HF) detector [7] shown in Figure 2. It includes two calorimeters HF+ and HF- which are located at a distance of 11.2 m on both sides from the IP5 and covering the pseudorapidity range $3 < |\eta| < 5$. The HF is a Cerenkov sampling calorimeter which uses radiation hard quartz fibers as the active material and steel plates as the absorber. It is azimuthally subdivided into 20^0 modular wedges, each of which consists of two azimuthal sectors of 10^0 . The detector fibers run parallel to the beamline and are bundled to form 0.175×1.175 ($\Delta\eta \times \Delta\phi$) towers. Half of the fibers run over the full depth of the absorber, whereas the other half starts at a depth of 22 cm from the front of the detector. These two sets of fibers are read out separately. Such a structure allows to distinguish showers generated

by electrons and photons, which deposit a large fraction of their energy in the first 22 cm, from those generated by hadrons, which produce signals in both calorimeter segments. The detector extends over 10 interaction lengths and includes 1200 towers in total. Its main physics objective is to measure the forward energy flow and forward jets.

The other CMS subcomponents that have been used to observe diffractive scattering in first minimum bias events are the ECAL and HCAL calorimeters covering the central region of CMS $-3 < \eta < 3$. These are the barrel and endcap detectors, which provide high-precision measurements of the energy of collision-products. The ECAL has an energy resolution of better than 0.5% above 100 GeV [8], while the HCAL, when combined with the ECAL, is able to measure the energy of hadrons with resolution of better than 10% above 300 GeV [9]. To trigger the CMS readout, two elements of the CMS detector monitoring system – the Beam Scintillator Counters (BSC) and the Beam Pick-up Timing for the eXperiments (BPTX) were used. The BSC devices are located at a distance of 10.86 m on both sides from the interaction point covering the pseudorapidity range $3.23 < |\eta| < 4.65$ and providing hit and coincidence signals with a time resolution of about 3 ns. Each BSC comprises 16 scintillator tiles. Two BPTX elements are located around the beam pipe at a distance of ± 175 m from the interaction point providing precise information on the bunch structure and timing of the incoming beam with a time resolution better than 0.2 ns.

III. EVENT SELECTION AND ACCEPTANCE

A search for diffractive events has been made as soon as the CMS detector has started to take collision data. In this paper, early observation of inclusive diffraction in minimum bias events collected by the CMS detector at $\sqrt{s} = 0.9$ TeV and 2.36 TeV in the fall of 2009 [10] is presented. To select a sample with the largest possible acceptance for SD events while suppressing beam-related background the following conditions were imposed. First, the presence of both beams was required by requesting the coincidence between BPTX signals in conjunction with a signal in one of the BSCs (the coincidence of the BSC signals was not required, since it would have obviously suppressed SD events). Then, to ensure that the selected event is a collision candidate, the events were required to have at least one primary vertex reconstructed from at least 3 tracks with a z distance to the interaction point below 15 cm and a transverse distance from the z -axis smaller than 2 cm. Further cuts were applied to reject beam-scraping and beam-halo events as well as events with large signals consistent with noise in the HCAL. Finally, the energy threshold in the calorimeters was set to 3 GeV, except for the HF where the threshold of 4 GeV was used. After applying all the requirements the number of selected events are 207345 and 11848 at $\sqrt{s} = 0.9$ TeV and 2.36 TeV, correspondingly.

To understand the effect of the applied selection cuts, the acceptance for SD events was studied as a function of the generated value of ξ – the fractional energy loss of the scattered proton, which in turn is the fraction of the incoming proton energy carried by the Pomeron. The corresponding distributions obtained with PYTHIA6 and PHOJET 1.12-35 generators for both collision energies are shown in Figure 3. The figure also illustrates the generator-level ξ distributions of SD events, which peak at low ξ values following roughly the $1/\xi$ dependence. As can be seen, there is a large discrepancy between the PYTHIA and PHOJET distributions which can be explained by the fact

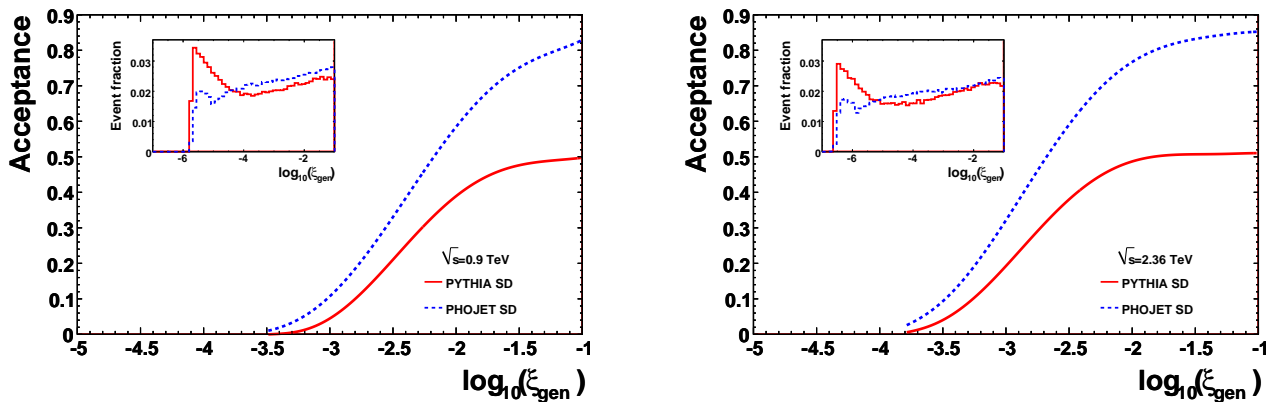


Figure 3: Acceptance for SD events obtained with PYTHIA and PHOJET after applying the selection cuts at $\sqrt{s} = 0.9$ TeV (left) and 2.36 TeV (right) as a function of the generated value of ξ . The generator-level ξ distributions are illustrated in the insert. The discrepancy between the generators is described in text.

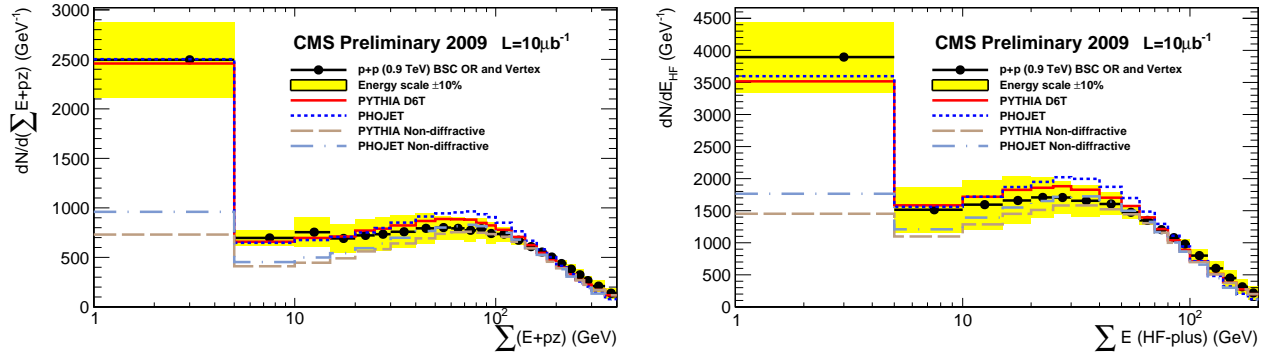


Figure 4: Distributions of the uncorrected variables $E + p_z$ (right) and E_{HF+} (left) at $\sqrt{s} = 0.9$ TeV. See text for details.

that the two generators model the diffractive contribution in a different way. In particular, PHOJET uses the Dual Parton Model [11] which describes diffractive processes by the interaction of the Pomeron with hadrons or another Pomeron. In this generator, the Pomeron exchange is represented as a mixture of soft and hard contributions, where the latter are described by perturbative QCD matrix elements. In contrast, PYTHIA6 does not include hard diffractive contributions and uses the Schuler-Sjöstrand model to describe the diffractive cross-sections and event characteristics [12]. Another explicit observation from the obtained distributions is a small acceptance for low- ξ events at both energies. To explain this feature one needs to take into account the fact that $\xi \sim M_X^2$, where M_X is the total mass of the diffractive system X . Obviously, the lighter the system X the harder to detect it experimentally. The selection efficiency for SD events is found to be about 35% according to PHOJET and about 20% according to PYTHIA, whereas for non-diffractive events it is approximately equal to 85% for both generators.

IV. OBSERVATION OF INCLUSIVE DIFFRACTION

Due to the presence of a LRG in the final state, SD events can be identified as those having no (or low) activity on one side of the forward region of CMS. As a result, the diffractive signal can be observed when plotting the selected events as a function of the energy deposition and tower multiplicity in the HF. Another variable giving an obvious evidence of the diffractive contribution is $E \pm p_z = \sum_i (E_i \pm p_{z,i})$, where E_i is the tower energy, $p_{z,i}$ is the longitudinal momentum and the sum runs over all calorimeter towers reconstructed in an event. The plus (minus) sign is assigned when the proton emitting the Pomeron moves in the $+z$ ($-z$) direction. Using energy and longitudinal momentum conservation it can be shown that this variable is roughly equal twice the Pomeron energy and therefore, is directly proportional to ξ . Taking into account the fact that the diffractive cross-section peaks at small ξ , diffractive events should cluster at low values of $E \pm p_z$. Figures 4 and 5 illustrate the distributions of the selected events as a function of $E + p_z$ and the energy deposition in the HF+, E_{HF+} , at $\sqrt{s} = 0.9$ TeV and 2.36 TeV, respectively. The other variable, the multiplicity of towers above threshold in the HF is shown in Figure 6 for both energies. As can clearly

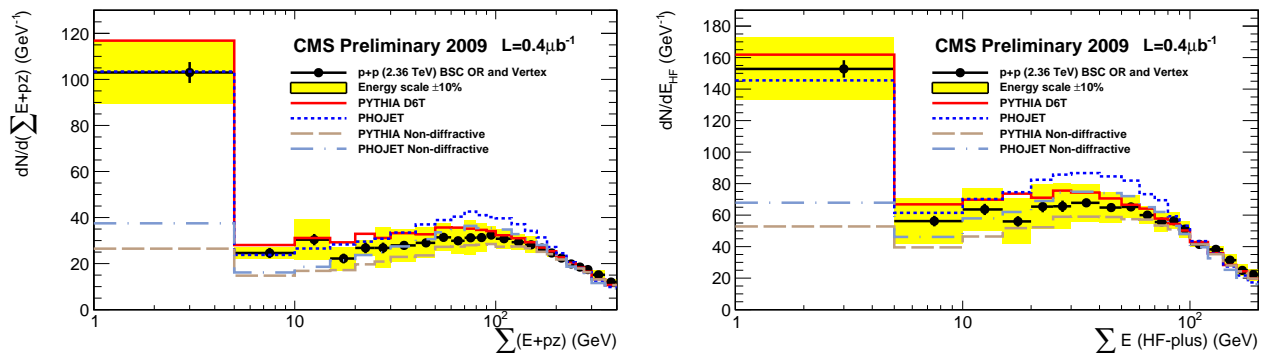


Figure 5: Distributions of the uncorrected variables $E + p_z$ (right) and E_{HF+} (left) at $\sqrt{s} = 2.36$ TeV. See text for details.

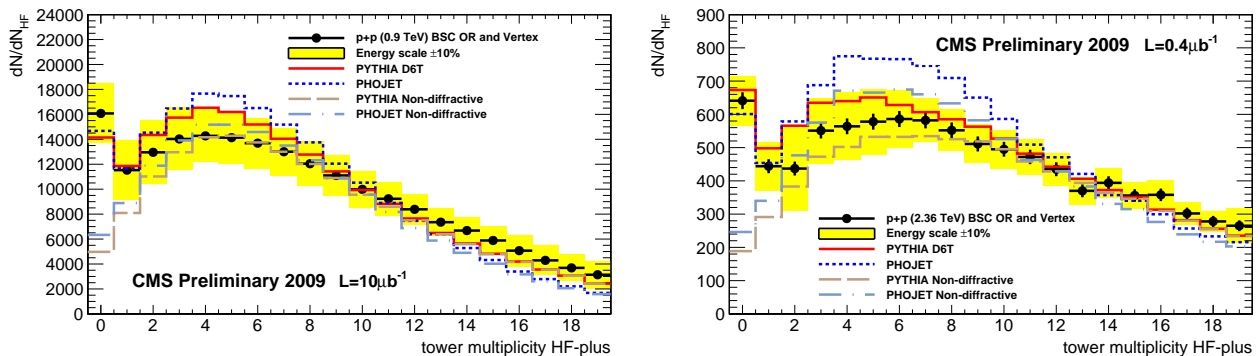


Figure 6: *Distribution of the uncorrected tower multiplicity in the HF+ at $\sqrt{s} = 0.9$ TeV (left) and 2.36 TeV (right) . See text for details.*

be seen, the diffractive signal peaks mainly in the first bin of the presented distributions. The vertical bars illustrate the statistical uncertainty of the data, whereas the bands demonstrate the main systematic uncertainty, which is due to the current imperfect calibration of the detectors and is estimated by a 10% variation of the energy scale. The corresponding PYTHIA and PHOJET predictions normalized to the data are also shown in these figures. As can be observed, there is a reasonable agreement between the data and Monte Carlo simulated events. In overall, PYTHIA describes the non-diffractive part of the spectra better than PHOJET. The predictions given by the generators without diffractive contribution are demonstrated in addition to strengthen the evidence of diffractive dissociation.

Figure 7 shows the distributions of $E - p_z$ and E_{HF-} at $\sqrt{s} = 0.9$ TeV after applying the cut to the energy sum in the HF+ to be below 8 GeV to enhance diffractive component in the data. This additional requirement allows to select mainly SD events with a LRG over HF+ boosting the system X towards the $-z$ direction. It can be seen that PHOJET agrees better with the data than PYTHIA after requiring $E_{HF+} < 8$ GeV particularly giving a better description of the high-mass diffractive systems. To complement the study, the selected events were also compared to the Monte Carlo predictions provided by three different PYTHIA6 tunes – D6T, DW and CW, which model multiple parton interactions in a different way. It was observed that the tunes give a similar overall description of the data. However, due to the present systematic uncertainties it is impossible to discriminate between the tunes.

V. OBSERVATION OF DIFFRACTIVE DI-JETS

One of the hard diffractive processes that have been observed by the CMS detector throughout 2010 in pp collisions at $\sqrt{s} = 7$ TeV is the SD production of di-jets, whose diagram is shown in Figure 8. As described in Section I, this is an interesting process to study due to its sensitivity to the rapidity gap survival probability and the gluon component of the proton dPDF. One of the first candidates of such a process recorded at $\sqrt{s} = 7$ TeV [13] is illustrated in

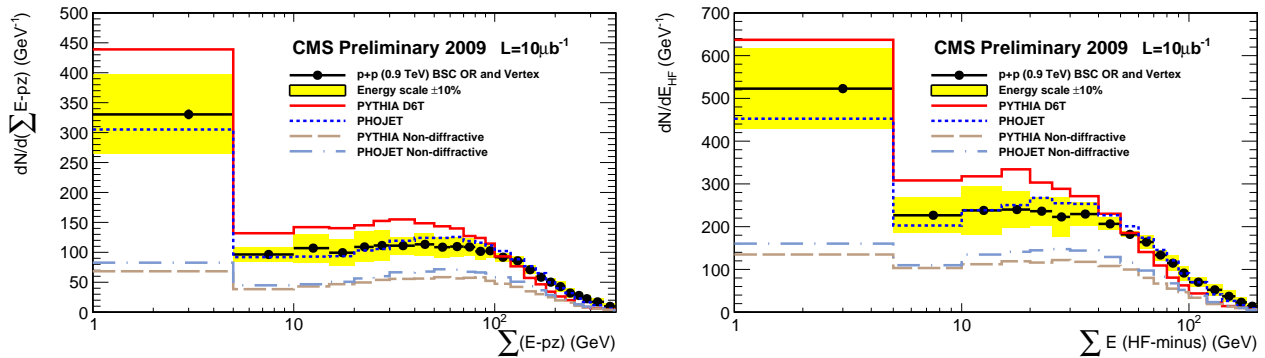


Figure 7: *Distributions of the uncorrected variables $E - p_z$ (left) and E_{HF-} (right) at $\sqrt{s} = 0.9$ TeV after applying the additional cut $E_{HF+} < 8$ GeV. See text for details.*

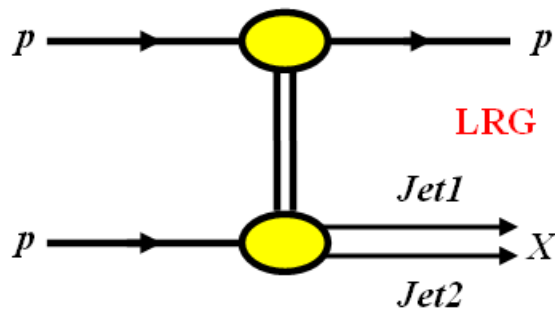


Figure 8: Sketch of the SD reaction $pp \rightarrow pX$, where X represents a di-jet system.

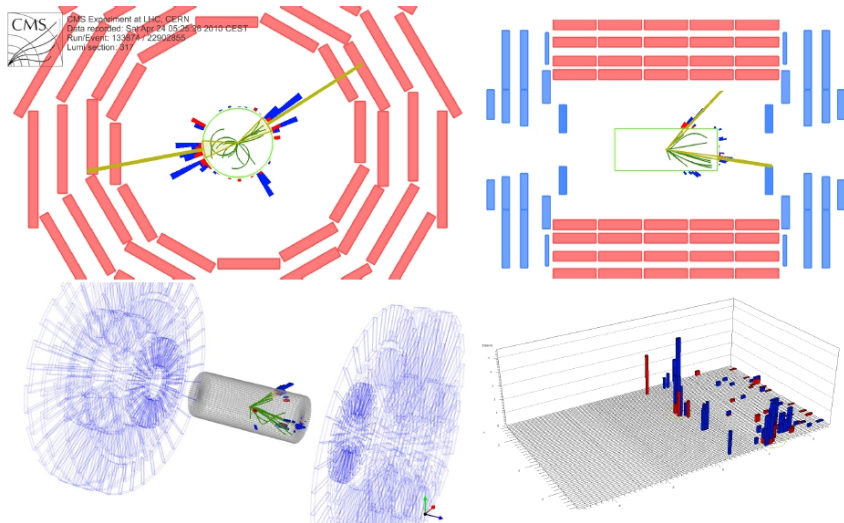


Figure 9: Display of an event with diffractive di-jet observed by the CMS detector at $\sqrt{s} = 7$ TeV.

Figure 9. The displayed event includes two jets – one with p_T of 43.5 GeV and η of 0.83 and the other with p_T of 36.9 GeV and η of 2.55, which both were reconstructed using the anti- k_t algorithm [14] with the radius parameter of 0.5. In this particular event, no energy deposition in the HF above 4 GeV is present. Moreover, it does not contain any activity in the region $\eta < 0$, which is a direct evidence of a LRG that extends over the $-z$ side of the CMS detector. This indicates the fact that the proton, which was traveling towards the $+z$ direction, dissociated into the two observed jets, whereas the other incoming proton escaped through the beam-pipe towards the $-z$ direction.

VI. CONCLUSIONS

Inclusive diffraction has been observed by the CMS detector in minimum bias events collected at $\sqrt{s} = 0.9$ TeV and 2.36 TeV. At both energies a clear diffractive contribution is evident. The data are compared to Monte Carlo predictions provided by PYTHIA6 and PHOJET generators. It is observed that PHOJET reproduces the diffractive contribution more accurately than PYTHIA6, whereas the latter gives a better description of the non-diffractive component of the data. In addition, first observation of di-jets created in consequence of the single-diffractive reaction in pp collisions at $\sqrt{s} = 7$ TeV is presented.

VII. ACKNOWLEDGMENTS

I would like to express my gratitudes to all people working in the CMS forward physics community. Special thanks go to Hannes Jung and Kerstin Borras for fruitful discussions, suggestions and encouragements.

-
- [1] *M. Deile et al.* Diffraction and Total Cross-Section at the Tevatron and the LHC. arXiv:hep-ex/0602021v1
 - [2] *P. Collins.* An Introduction to Regge Theory and High-Energy Physics, Cambridge University Press, 1977.
 - [3] *B. Cox et al.* Phys.Comm. 144, 104 (2002); *V. Khoze et al.* arXiv:0802.0177 [hep-ph]
 - [4] *CMS Collaboration.* CERN CMS-PAS-DIF-07-002 (2007).
 - [5] *CMS Collaboration.* CERN CMS-PAS-FWD-08-002 (2008).
 - [6] *CMS Collaboration.* The CMS Experiment at the CERN LHC, 2008 JINST 3 S8004.
 - [7] *A. Penzo et al.* The CMS-HF quartz fiber calorimeters, 2009 J. Phys.: Conf. Ser. 160 012014.
 - [8] *R.M. Brown.* The CMS lead tungstate electromagnetic calorimeter, 2008 J. Phys.: Conf. Ser. 110 092005.
 - [9] *S. Sharma.* Understanding the performance of CMS calorimeter, Pramana, vol. 69, issue 6, (2007) 1069-1074.
 - [10] *CMS Collaboration.* CERN CMS-PAS-FWD-10-001 (2010).
 - [11] *A. Capella et al.* Dual parton model, Phys. Rep. 236, 225 (1994).
 - [12] *S. Navin.* Diffraction in Pythia, arXiv:1005.3894v1 [hep-ph].
 - [13] *CMS Collaboration.* CERN CMS DPS-2010/036 (2010).
 - [14] *M. Cacciari et al.* The anti- k_t jet clustering algorithm, JHEP04(2008)063.